J. Phys. Chem. **1981,** *85,* 575–579

Transfer of Hydrogen by Hydroaromatics. 2. The Temperature Dependence of the Rate Constants and Catalytic Site Populations in the Tetralin/Iron Catalyst Systems

T. E. Gangwer

Brookhaven National Laboratory, Associated Universities, Inc., Upton, New York 11973 *(Received: August 5, 1980)*

The heterogeneous mechanism of dehydrogenation for the tetralin/iron catalyst system previously reported is further documented. The temperature dependences of the rate constants are reported. The effective activation energies on these heterogeneous surfaces were found to be in the −20 to +30 kcal/mol range. The catalytic site populations and temperature dependences were used to determine the binding energy, E_b, of the organic reactants at the catalytic sites. The E_b values were found to be in the 20–40 kcal/mol range.

Introduction

The chemistry of hydrogen donation by hydroaromatics is of interest to a number of fields of investigation ranging from basic studies of organic synthesis,[1-6] chemical kinetics and mechanisms,[7-13] to applied work in coal liquefaction. These studies cover reaction conditions ranging from gas to condensed phase and simple to complex chemical mixtures. The net chemical process carried out by hydroaromatics during the hydrogenation of organic materials is the transfer of hydrogen, present as molecular hydrogen H_2, to the organic system. In order to gain insight into this hydrogen transfer process, we are investigating the basic dehydrogenation/hydrogenation chemistry of hydroaromatic systems at this laboratory.

The tetralin hydroaromatic system has been previously shown to undergo dehydrogenation/hydrogenation via a heterogeneous, first-order process. The rate-limiting reactions undergone by the tetralin/1,2-dihydronaphthalene/naphthalene/H_2 species which comprise this system take place on the heterogeneous surfaces present in the reaction vessels.[7] The detailed mechanism and kinetic treatment for tetralin/iron catalyst systems at 400 °C has been reported.[8] This kinetic interpretation[8] gave rate expressions which yielded rate constants and reactive site populations. The present study reports the observed temperature dependence of these rate constants and surface populations for the same tetralin/iron catalyst systems.

Experimental Section

The tetralin, obtained from Aldrich Chemical, was 99.4% pure (the main impurity being 0.4% naphthalene) and was used as received. The iron(III) oxide (Fe_2O_3) was from the Baker Chemical Co. The limonite ($2Fe_2O_3{\cdot}3H_2O$), magnetite (Fe_3O_4), and pyrite (FeS_2) catalysts were purchased from Ward's Scientific Co. The catalysts were ground and sieved such that only those solids which were ~37 μm or less were used. The experimental equipment and procedures are the same as previously reported.[8] Briefly, the reactions were run in evacuated quartz vessels containing 100 mg of catalyst and ~90 μL of tetralin. Each reaction vessel was placed in an oven set at the reacting temperature. The vessels reached reacting temperature within 5 min. After the given reaction time, the vessel was removed and rapidly chilled to room temperature by plunging it into water. Benzene extracts of the reaction mixtures in each vessel were analyzed on a gas chromatograph by using flame ionization detection and dual 6-ft Durapak K (Carbowax 400–Porasil F) $^1/_8$-in. columns. The GC data were analyzed by using an integrator and are reported as area percent. The tetralin and naphthalene analyses were reproducible to within 1% of the reported area percent values. The 1,2-dihydronaphthalene analysis was not as reproducible (12% of the observed area percent values) because this species eluted on the shoulder of the much larger tetralin peak.

Results

Figures 1–3 show[17] the kinetic data (% conversion per 100 mg of catalyst) for tetralin (T) and the two main organic products 1,2-dihydronaphthalene (D) and naphthalene (N). The mechanistic fits to the data shown in these figures are based on the rate-limiting reactions

$$T/S_\eta \xrightarrow{k_1} D/(S/H)_\eta \qquad (1)$$

$$D/S_\eta' \xrightarrow{k_2} N/(S'/H)_\eta \qquad (2)$$

$$D/(S/H)_\eta \xrightarrow{k_3} T/S_\eta \qquad (3)$$

$$N/(S'/H)_\eta \xrightarrow{k_4} D/S_\eta' \qquad (4)$$

where the slanted line (/) denotes site binding and $(S/H)_\eta$ or $(S'/H)_\eta$ denotes reactive S_η or S_η' sites which have gained hydrogen atoms. The tetralin oxidation (reaction 1)/1,2-dihydronaphthalene reduction (reaction 3) catalytic sites

---

(1) Brieger, G.; Lestrick, T. J. *Chem. Rev.* **1974**, *74*, 567.
(2) Lu, P. P.; Harvey, R. G. *Chem. Rev.* **1978**, *78*, 317.
(3) Maslovich, N. L.; Artemov, A. V.; Seleznev, V. A.; Sysoeva, N. A.; Krylov, O. V. *Kinet. Catal.* **1978**, *19*, 418.
(4) Dimitrova, R. P.; Dimitrov, Chr. *React. Kinet. Catal. Lett.* **1979**, *10*, 143.
(5) Chao, C. C.; Hart, D. W.; Bau, R.; Heck, R. F. J. *Organometal. Chem.* **1979**, *179*, 301.
(6) Mizukami, F.; Horiguchi, Y.; Tajima, M.; Imamura, *J. Bull. Chem. Soc. Jpn.* **1979**, *52*, 2689.
(7) Gangwer, T.; MacKenzie, D.; Casano, S. *J. Phys. Chem.* **1979**, *83*, 2013.
(8) Gangwer, T. *J. Phys. Chem.* **1980**, *84*, 2436.
(9) van der Jagt, P. J.; de Haan, H. K.; van Zanten, B. *Tetrahedron* **1971**, *27*, 3207.
(10) Cronauer, D. C.; Jewell, D. M.; Shah, Y. T.; Modi, R. J.; Seshadri, K. S. *Ind. Eng. Chem. Fundam.* **1979**, *18*, 368.
(11) Collins, C. J.; Raaen, F. V.; Benjamin, B. M.; Maupin, P. H.; Roark, W. H. *J. Am. Chem. Soc.* **1979**, *101*, 5009.
(12) Levsen, K.; Borchers, F.; Stolze, R.; Budzikiewiez, H. *Org. Mass. Spectrosc.* **1978**, *13*, 510.
(13) Prasad, K. M.; Athappan, R.; Srivastava, R. D. *J. Catal.* **1979**, *59*, 460.
(14) Adamson, A. W. "Physical Chemistry of Surfaces", 2nd ed.; Interscience: New York, 1967; Chapter XIII.
(15) Holmes, J. M. In "The Solid-Gas Interface"; Flood, E. A.; Ed.; Marcel Dekker: New York, 1967; Chapter 5.
(16) Smol, B.; Gangwer, T., unpublished data.
(17) Figures 2–8 are available as supplementary material. See paragraph at end of text.

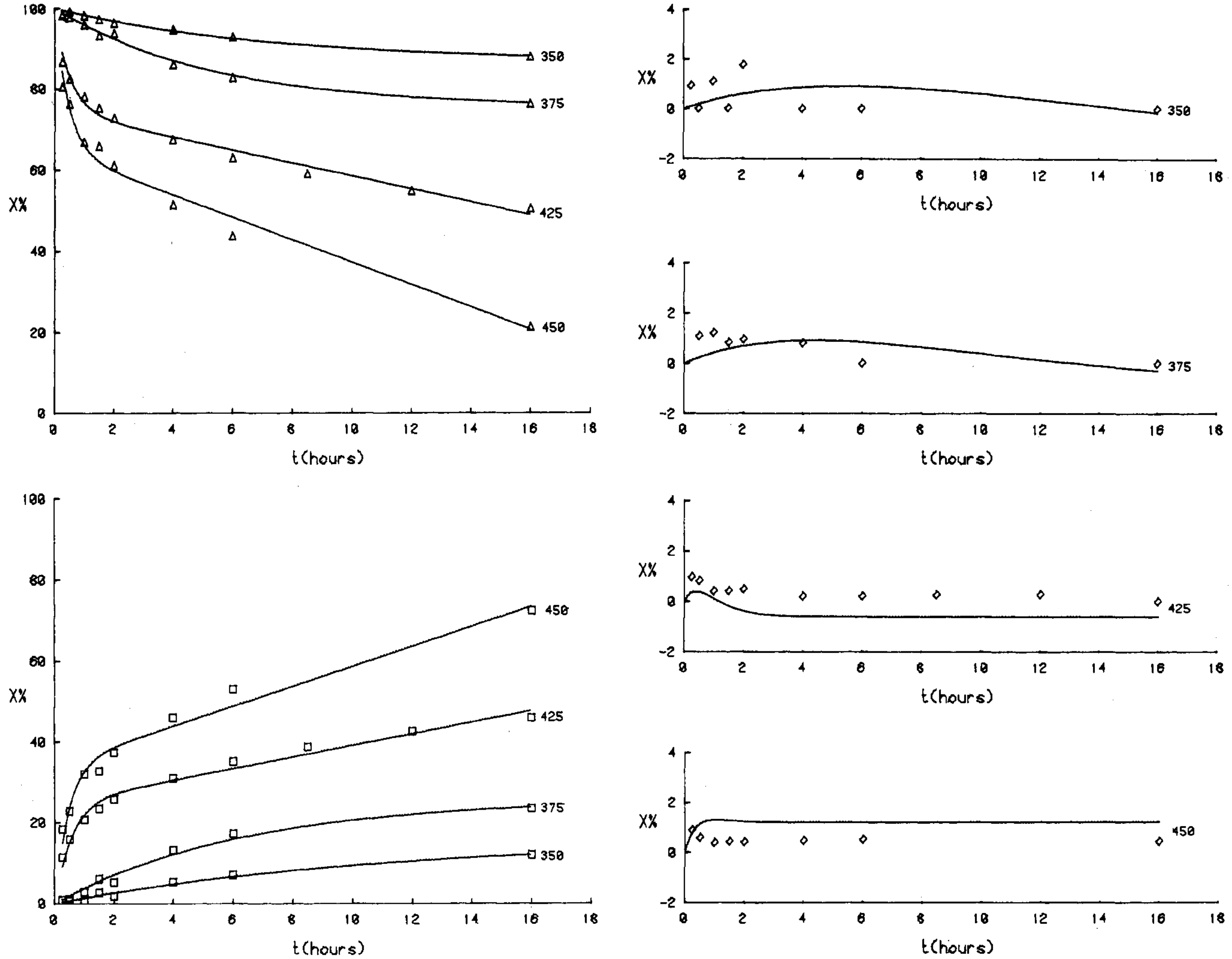

Figure 1. The time dependence of the extents of reaction (% conversion per 100 mg of catalyst) for tetralin dehydrogenation (△) and naphthalene (◇) and 1,2-dihydronaphthalene (□) formation over the 350–450 °C temperature range for the Fe_2O_3 catalytic system. The solid lines are the analytic fits to the experimental data based on eq I–III. The 400 °C data are not included since they have been previously reported.

are denoted by S_η and the 1,2-dihydronaphthalene oxidation (reaction 2)/naphthalene reduction (reaction 4) catalytic sites are denoted by S_η'. The rate equations which describe the mechanistic fit are

$$X_T = 100 - \frac{P_{11}'}{A_T^2}G(1 - e^{-A_T t}) - \frac{P_{13}'}{A_T}Gt \qquad \text{(I)}$$

$$X_N = \frac{P_{22}'}{A_N^2}G(1 - e^{-A_N t}) + \frac{P_{24}'}{A_N}Gt \qquad \text{(II)}$$

$$X_D = \frac{P_{11}'}{A_T^2}G(1 - e^{-A_T t}) - \frac{P_{22}'}{A_N^2}G(1 - e^{-A_N t}) + \left(\frac{P_{13}'}{A_T} - \frac{P_{24}'}{A_N}\right)Gt \qquad \text{(III)}$$

where

$$X_T = \frac{[T]}{T_0}100 \qquad X_N = \frac{[N]}{T_0}100 \qquad X_D = \frac{[D]}{T_0}100$$

$$P_{11}' = \frac{k_1^2 C_{13} 10^2}{T_0 G} \qquad P_{13}' = \frac{k_1 k_3 C_{13} 10^2}{T_0 G}$$

$$P_{22}' = \frac{k_2^2 C_{24} 10^2}{T_0 G} \qquad P_{24}' = \frac{k_2 k_4 C_{24} 10^2}{T_0 G}$$

$$C_{13} = [T/S_\eta] + [D/(S/H)_\eta]$$

$$C_{24} = [D/S_\eta] + [N/(S'/H)_\eta]$$

C_{13} and C_{24} are the surface coverages of the S_η and S_η' sites, G is the grams of catalyst (i.e., 0.100 g in the present study), t is reaction time in hours, the brackets denote concentration, and T_0 is the total concentration of organic present in the reaction vessel (i.e., 6.81×10^{-4} mol in the present study). The detailed derivation of these rate expressions has been previously reported.[8] The following assumptions and conclusions, which are based on experimental observations,[8] apply to these rate expressions: (1) The rate-limiting steps are heterogeneous, first-order reactions. (2) Surface absorption/desorption of reactants and products is rapid with respect to the rate-limiting steps. (3) Rapid migration of H species occurs on the surface. (4) Under the conditions studied, readsorption of H_2 to yield H species is not a significant process. (5) The net S_η and S_η' surface coverages, denoted by C_{13} and C_{24}, are constants with respect to time.

Table I lists the rate parameters for eq I–III obtained from the nonlinear least-squares analysis of the data. The solid lines in Figures 1–3 for tetralin and naphthalene show[17] the nonlinear least-squares fit to these data. The solid line in the 1,2-dihydronaphthalene was calculated by using the rate parameters obtained from the tetralin and naphthalene analysis with no parameter adjustment. The agreement between the observed data and the proposed mechanism is well within the experimental reproducibility.

Table II lists the rate constants terms for the four iron catalysts obtained from the parameters in Table I by using

TABLE I: Rate Parameters and Standard Deviations for Eq I-III

catalyst	T, °C	A_t, h^{-1}	$\sigma(A_t)$	$10^{-2}P'_{11}$, %/g h^{-2}	$10^{-2}\cdot\sigma(P'_{11})$	$10^{-2}\cdot P'_{13}$, %/g h^{-2}	$10^{-2}\cdot\sigma(P'_{13})$	A_N, h^{-1}	$\sigma(A_N)$	$10^{-2}P'_{22}$, %/g h^{-2}	$10^{-2}\cdot\sigma(P'_{22})$	$10^{-2}\cdot P'_{24}$, %/g h^{-2}	$10^{-2}\cdot\sigma(P'_{24})$
Fe_2O_3	450	2.22	0.02	17.4	0.5	0.613	0.007	2.16	0.02	15.9	0.5	0.534	0.006
	425	1.91	0.02	8.86	0.30	0.306	0.005	1.76	0.02	7.68	0.26	0.253	0.004
	400	1.16	0.01	2.65	0.11	0.111	0.003	0.984	0.011	1.93	0.09	0.0867	0.0021
	375	0.188	0.002	0.088	0.011			0.159	0.002	0.0655	0.0091		
	350	0.141	0.004	0.0264	0.0032			0.0936	0.0033	0.0137	0.0021		
limonite	450	4.33	0.01	161	3	0.740	0.010	4.13	0.01	145	3	0.710	0.010
	425	2.11	0.01	27.4	0.9	0.367	0.004	1.92	0.01	22.6	0.8	0.326	0.003
	400	1.33	0.01	8.76	0.36	0.222	0.003	1.18	0.01	6.82	0.31	0.191	0.002
	375	0.859	0.006	2.71	0.14	0.139	0.002	0.721	0.005	1.96	0.12	0.107	0.002
magnetite	450	1.39	0.02	3.13	0.14	0.357	0.008	0.914	0.015	1.30	0.07	0.175	0.004
	437	1.36	0.02	2.59	0.13	0.257	0.006	0.721	0.015	0.645	0.043	0.105	0.003
	425	1.44	0.04	1.95	0.13	0.179	0.006	0.834	0.023	0.641	0.050	0.0813	0.0034
	400	2.94	0.11	5.41	0.46	0.193	0.010	1.44	0.07	0.94	0.11	0.0864	0.0057
	375	4.49	0.28	8.8	1.2	0.153	0.013	2.01	0.18	1.05	0.22	0.0647	0.0077
pyrite	425	2.65	0.06	7.58	0.41	0.959	0.025	1.30	0.03	1.99	0.11	0.306	0.008
	400	3.48	0.16	6.31	0.65	0.341	0.019	1.27	0.08	0.590	0.095	0.103	0.008
	375	5.29	0.42	10.0	1.7	0.206	0.020	1.94	0.20	0.78	0.19	0.0677	0.0085

TABLE II: Rate Constants and Standard Deviations for Reaction 1-4

catalyst	T, °C	10^4k_1, s^{-1}	$10^4\sigma(k_1)$	10^4k_2, s^{-1}	$10^4\sigma(k_2)$	10^5k_3, s^{-1}	$10^5\sigma(k_3)$	10^5k_4, s^{-1}	$10^5\sigma(k_4)$
Fe_2O_3	450	5.96	0.07	5.81	0.07	2.10	0.10	1.95	0.10
	425	5.13	0.07	4.73	0.07	1.77	0.11	1.56	0.10
	400	3.09	0.04	2.62	0.04	1.30	0.10	1.18	0.10
	375	0.522	0.006	0.442	0.006				
	350	0.392	0.011	0.260	0.009				
limonite	450	12.0	0.03	11.4	0.03	0.550	0.019	0.559	0.021
	425	5.78	0.03	5.26	0.03	0.775	0.038	0.758	0.038
	400	3.60	0.03	3.19	0.03	0.913	0.057	0.893	0.058
	375	2.27	0.03	1.90	0.03	1.16	0.09	1.04	0.090
magnetite	450	3.47	0.09	2.24	0.07	3.95	0.32	3.01	0.28
	437	3.44	0.09	1.72	0.07	3.41	0.30	2.80	0.33
	425	3.66	0.15	2.06	0.10	3.36	0.43	2.61	0.38
	400	7.89	0.35	3.66	0.27	2.81	0.49	3.37	0.78
	375	12.3	0.8	5.26	0.64	2.13	0.60	3.2	1.4
pyrite	425	6.53	0.25	3.13	0.13	8.27	0.85	4.81	0.50
	400	9.17	0.54	3.00	0.38	5.0	1.0	5.2	1.6
	375	14.4	1.3	4.96	0.76	3.0	1.0	4.3	2.0

the previously reported[8] relationships between A_T, P_{11}', and P_{13}':

$$k_3 = \frac{A_T}{(P_{11}'/P_{13}' + 1)}$$

$$k_1 = A_T - k_3$$

and between A_N, P_{22}', and P_{24}'

$$k_4 = \frac{A_N}{(P_{22}'/P_{24}' + 1)}$$

$$k_2 = A_N - k_4$$

The temperature range studied (mainly 375–450 °C) was constrained by the lack of reactivity below 375 °C and the onset of pyrolytic chemistry above 450 °C. Thus at 350 °C the net tetralin conversion rate is quite slow as shown in Figure 1 for the Fe_2O_3 system and therefore was not studied in detail for the other systems. At temperatures above 400 °C the formation of the previously minor (i.e., <1.0%) product methylindane begins to increase. Experiments on the 450 °C pyrite system showed that the methylindane yield gets as high as 22% of the product mix. The mechanistic analysis of the 450 °C pyrite data does not yield rate constants and surface populations which agree with the temperature dependencies of the parameters obtained for the other systems or the lower temperature pyrite studies. Because the additional chemistry which is responsible for the large methylindane yield in the 450 °C pyrite system is not significant in the remaining systems, the 450 °C pyrite data will not be presented here. The formation of methylindane is known to increase at 400 °C as one progresses toward the condensed phase. The role of methylindane formation is an aspect of the chemistry of the tetralin system which is currently being pursued. For the results presented here, the formation of methylindane can be treated as a minor reaction pathway.

Table III lists the surface site populations (M_{13} and M_{24}) determined by using the previously reported[8] relationships

$$M_{13} = C_{13}/S_0$$

$$M_{24} = C_{24}/S_0$$

where S_0 is the BET surface area of the heterogeneous solids. The results in this table are normalized since all the surface areas S_0 were determined by using argon as the adsorbent. The total site population M given in Table III is just

$$M = M_{13} + M_{24}$$

Discussion

The present mechanism treats the heterogeneous system as going through the following sequence of events: (1)

TABLE III: Surface Site Populations and Standard Deviations Based on the Kinetic Analysis and Measured Surface Areas S_0 for the Catalytic Systems

catalyst, S_0(m^2/g)	T, °C	$10^{-13}M_{13}$, molecule/cm^2	$10^{-13}\sigma(M_{13})$	$10^{-13}M_{24}$, molecule/cm^2	$10^{-13}\sigma(M_{24})$	$10^{-13}M$, molecule/cm^2
Fe_2O_3, 9.76 ± 0.78	450	15.9	2.2	15.3	2.1	31.2
	425	10.9	1.6	11.1	1.6	22.0
	400	9.0	1.4	9.1	1.5	18.1
	375	10.4		10.9		21.3
	350	5.60		6.57		12.2
limonite, 82.68 ± 0.36	450	4.30	0.15	4.26	0.15	8.56
	425	3.14	0.17	3.13	0.18	6.27
	400	2.58	0.18	2.57	0.20	5.15
	375	2.01	0.17	2.08	0.20	4.09
magnetite, 6.30 ± 0.03	450	13.1	1.4	13.0	1.7	26.1
	437	11.0	1.2	10.9	1.8	21.9
	425	7.3	1.2	7.6	1.4	14.9
	400	4.37	0.81	3.52	0.97	7.89
	375	2.94	0.83	1.91	0.88	4.85
pyrite, 2.19 ± 0.11	425	25.6	4.8	29.3	5.8	54.9
	400	10.8	3.0	9.5	4.4	20.3
	375	7.0	2.8	4.6	2.8	11.6

TABLE IV: Activation and Binding Energies (kcal/mol) for Reactions 1-4

catalyst	reaction	E_e	$\sigma(E_e)$	$(E_b - Q)$	$\sigma(E_b - Q)$	E_b	E_c
Fe_2O_3	1	+27.8	5.2	6.8	2.1	22	50
	2	+30.9	4.9				53
	3	+9.3	1.4				31
	4	+9.72	0.43				32
limonite	1	+20.3	2.2	8.96	0.78	24	44
	2	+21.8	2.2				46
	3	−8.9	1.1				15
	4	−7.4	1.4				17
magnetite	1	−17.6	2.6	21.8	1.2	37	19
	2	−13.1	3.2				24
	3	+7.24	0.66				44
	4	−1.8	1.5				35
pyrite	1	−14.2	0.85	27.8	5.1	43	29
	2	−8.4	5.5				35
	3	+18.2	0.31				61
	4	+2.1	2.7				45

adsorption/desorption between the reactant and the general heterogeneous surface (S_0, Q); (2) reactant migration between catalytic sites S where reversible reactant/site complexing occurs (M, E_b); (3) conversion of the reactant/site complex to product/site complex (k, E_c); (4) continuation of the cycle where now the products become reactants and thus set up competition for the catalytic sites. Here the kinetic and thermochemical parameters determined for each step are given in parentheses. The basis for the second and fourth steps in the sequence is observed chemistry. The net disproportionation of 1,2-dihydronaphthalene[7] and hydrogenation of naphthalene observed for these catalytic systems[16] clearly shows that the tetralin products are reactants in the system. The incorporation of these two steps in the mechanism is accomplished by defining C_{13} and C_{24} in accordance with reactions 1–4. One measure of the utility of the proposed mechanism in describing the observed kinetic behavior is demonstrated by the success of the rate eq I–IV in describing the experimental data (i.e., Figures 1–3).[17] A second indication of the applicability of the mechanism is the observed consistancy in the interpretations of the temperature dependencies of the calculated rate constants and surface populations as discussed below.

For a given heterogeneous reaction sequence, where the rate-limiting reactions take place on the surface, the activation process involves the binding of the reactant at the catalytic site. This binding, which is a function of the catalytic system, lowers the energy required for the subsequent conversion to products. Thus the temperature dependence of the rate constants is

$$k = Ae^{-E_e/RT} \qquad \text{(IV)}$$

where the effective activation energy on the surface E_e is defined as the catalytic site activation energy for conversion E_c minus the binding energy of the catalytic site E_b

$$E_e = E_c - E_b \qquad \text{(V)}$$

That is, the potential energy surface for a reaction in the tetralin system is being treated as having a reactant catalytic site barrier whose height (i.e., activation energy) is a function of the nature of the binding of the reactant to the heterogeneous site. The energy of binding of the reactant on a heterogeneous site E_b is therefore viewed as effecting a change in the potential energy barrier (i.e., E_c) between reactant and product. As is evident from the dependence given by eq V, the relative magnetudes of E_b and E_c will determine whether the effective activation energy, E_e, is positive or negative.

The Arrhenius type rate constant/temperature plots in Figures 4–7 show[17] good linearity and the resultant E_e values are given in Table IV. The k_1 and k_2 for pyrite, k_3 and k_4 for limonite, and k_1, k_2, and k_4 for magnetite show temperature dependencies that yield negative effective surface activation energies. As discussed above this is a result of the binding energy being greater than the surface activation energy for conversion. Thus for a negative effective activation energy the decrease in reactivity with temperature for these systems is attributed to the binding of the reactant to the catalytic surface site.

The binding of a reactant on the surface of a solid R_s to a catalytic site S can be treated as the equilibrium process

$$R_s + S \underset{k_6}{\overset{k_5}{\rightleftharpoons}} R/S \qquad (5,6)$$

where R/S is the reactant/catalytic site complex. Now for this equilibrium process we know that

$$\frac{k_5}{k_6} = \frac{[R/S]}{[R_s][S]}$$

or equivalently

$$[R/S] = S_0[S]\theta\frac{k_5}{k_6} \qquad (VI)$$

where θ is defined as the fractional surface coverage of the total available surface area S_0 of the heterogeneous solid and the brackets denote concentration. For Langmuir adsorption[14] at low coverage

$$\theta = bP = Pb_0(T)^{-1/2}e^{Q/RT} \qquad (VII)$$

where Q is the energy of adsorption on to the surface, P is the pressure of reactant in the gas phase, and b_0 is a product of constants. Substituting the temperature-dependent expressions of the rate constants and θ into eq VI gives

$$[R/S] = S_0[S]Pb_0(T)^{-1/2}e^{Q/RT}\frac{A_5}{A_6}e^{-(E_5-E_6)/RT}$$

which simplifies to

$$M_r = A(T)^{1/2}e^{-(E_b-Q)/RT} \qquad (VIII)$$

since, by definition

$$M_r = [R/S]/S_0$$

and, by convention

$$E_b = E_5 - E_6$$

$$P = \frac{\eta R}{V}T$$

The product of the preexponential terms is defined as the constant A which is independent of temperature (note at low coverage [S] will be temperature independent).

As shown[17] in Figure 8 a plot of the ln M from Table III vs. T^{-1} gives a linear plot. Now M is the sum of the surface site populations for the species given in reactions 1–4:

$$M = M_1 + M_2 + M_3 + M_4$$

where

$$M_1 = [T/S_\eta]/S_0 \qquad M_2 = [D/S_\eta']/S_0$$

$$M_3 = [D/(S/H)_\eta]/S_0 \qquad M_4 = [N/(S'/H)_\eta]/S_0$$

If, for eq VIII, these four species have comparable exponential terms

$$M = (A_1 + A_2 + A_3 + A_4)(T)^{1/2}e^{-(E_b-Q)/RT}$$

or

$$M = Ae^{-(E_b-Q)/RT} \qquad (IX)$$

where the $(T)^{1/2}$ dependence of the A term can be ignored for the limited temperature range studied.

The heats of adsorption for benzene and cyclohexane on a diverse range of surfaces are consistantly in the 9–10 kcal/mol range.[15] The adsorption energy Q for the organics in the tetralin systems is taken to be ~15 kcal/mol where it is assumed that both rings of these naphthalenic systems partially contribute to yield this average value. Based on this assumed value, one can calculate E_b from the slopes $(E_b - Q)$ of the lines in Figure 8[17] which are plots based on eq IX. The slopes and resultant E_b values are given in Table IV. The E_b values show that the complexing of the organics by the catalytic sites is comparable in the Fe_2O_3 and limonite systems and strongest for the pyrite system. A competition for the reactive sites takes place among the tetralin, 1,2-dihydronaphthalene, and naphthalene reactants migrating over the surface of a given catalyst. Information on the steady-state composition of M could be determined if the individual Q and E_b values for these three organic reactants were known.

Based on the E_b values derived from the surface site populations, the values for E_c given in Table IV were obtained by using eq 5. The fact that this adjustment in E_e, for the lowering of the energy required for reaction due to binding, yields positive values for the catalytic site activation energy for conversion E_c is taken as evidence supporting the mechanism. Based on these E_c values, the oxidation reactions 1 and 2 are most effectively catalyzed by the magnetite system and least effectively by the iron oxide system. The reduction reactions 3 and 4 are most effectively catalyzed by the limonite system and least effectively by the pyrite system. Clearly, the numerical value of E_c is quite sensitive to the nature of the four catalysts for a given reaction and to the four conversion processes for a given catalyst. Based on steric/coordination arguments, one can propose an explanation of this variability in E_c. Reactant/product steric considerations, based on known chemistry of closely related decalin systems and on the fact that conversion between tetralin and naphthalene involves 1,2-dihydronaphthalene but not 1,4-dihydronaphthalene, have previously been interpreted[8] as indicating that the fixation of a reactant in these systems requires a minimum coordination of three at the catalytic site. It is proposed that the process of achieving such multicoordinated site fixation for these polycyclic aromatic ring systems will be quite sensitive to the surface geometry requirements which are specific to each reaction/catalyst combination.

With respect to the surface populations, the experimentally observed temperature dependence of M is taken as evidence that the formation of the reactive catalytic site population is a process which requires surmounting an activation barrier (i.e., E_5). If the surface population of catalytic sites was determined only by the adsorption/desorption processes between the gas and solid phases (i.e., Q), the value of M should decrease as the temperature is increased according to eq VII. Introduction of the activated processes of the chemical equilibrium defined by reactions 5 and 6 provides an interpretation of the M temperature dependence.

Acknowledgment. This work was supported by the Division of Chemical Sciences, U.S. Department of Energy, Washington, D.C., under Contract No. DE-AC02-76CH00016.

Supplementary Material Available: Figures 2 and 3, showing the data/mechanism fits for the limonite, magnetite, and pyrite systems, and Figures 4–8, showing the linearized k and M temperature dependencies for the four catalyst systems (7 pages). Ordering information is available on any current masthead page.